

# UCSF

## UC San Francisco Previously Published Works

### Title

Relative contribution of TARPs  $\gamma$ -2 and  $\gamma$ -7 to cerebellar excitatory synaptic transmission and motor behavior

### Permalink

<https://escholarship.org/uc/item/2fn5c0fh>

### Journal

Proceedings of the National Academy of Sciences of the United States of America, 112(4)

### ISSN

0027-8424

### Authors

Yamazaki, Maya  
Le Pichon, Claire E  
Jackson, Alexander C  
et al.

### Publication Date

2015-01-27

### DOI

10.1073/pnas.1423670112

Peer reviewed

# Relative contribution of TARPs $\gamma$ -2 and $\gamma$ -7 to cerebellar excitatory synaptic transmission and motor behavior

Maya Yamazaki<sup>a,b,1</sup>, Claire E. Le Pichon<sup>c,1,2</sup>, Alexander C. Jackson<sup>a,1,3,4</sup>, Manuel Cerpas<sup>a</sup>, Kenji Sakimura<sup>b</sup>, Kimberly Scarce-Levie<sup>c</sup>, and Roger A. Nicoll<sup>a,d,4</sup>

<sup>a</sup>Department of Cellular and Molecular Pharmacology, <sup>d</sup>Department of Physiology, University of California, San Francisco, CA 94143; <sup>b</sup>Department of Cellular Neurobiology, Brain Research Institute, Niigata University, Niigata, 951-8585, Japan; and <sup>c</sup>Department of Neuroscience, Genentech, South San Francisco, CA 94080

Contributed by Roger A. Nicoll, December 18, 2014 (sent for review November 4, 2014)

**Transmembrane AMPA receptor regulatory proteins (TARPs) play an essential role in excitatory synaptic transmission throughout the central nervous system (CNS) and exhibit subtype-specific effects on AMPA receptor (AMPA) trafficking, gating, and pharmacology. The function of TARPs has largely been determined through work on canonical type I TARPs such as stargazin (TARP  $\gamma$ -2), absent in the ataxic *stargazer* mouse. Little is known about the function of atypical type II TARPs, such as TARP  $\gamma$ -7, which exhibits variable effects on AMPAR function. Because  $\gamma$ -2 and  $\gamma$ -7 are both strongly expressed in multiple cell types in the cerebellum, we examined the relative contribution of  $\gamma$ -2 and  $\gamma$ -7 to both synaptic transmission in the cerebellum and motor behavior by using both the *stargazer* mouse and a  $\gamma$ -7 knockout (KO) mouse. We found that the loss of  $\gamma$ -7 alone had little effect on climbing fiber (cf) responses in Purkinje neurons (PCs), yet the additional loss of  $\gamma$ -2 all but abolished cf responses. In contrast,  $\gamma$ -7 failed to make a significant contribution to excitatory transmission in stellate cells and granule cells. In addition, we generated a PC-specific deletion of  $\gamma$ -2, with and without  $\gamma$ -7 KO background, to examine the relative contribution of  $\gamma$ -2 and  $\gamma$ -7 to PC-dependent motor behavior. Selective deletion of  $\gamma$ -2 in PCs had little effect on motor behavior, yet the additional loss of  $\gamma$ -7 resulted in a severe disruption in motor behavior. Thus,  $\gamma$ -7 is capable of supporting a component of excitatory transmission in PCs, sufficient to maintain essentially normal motor behavior, in the absence of  $\gamma$ -2.**

cerebellum | AMPA receptors | TARPs | *stargazer* | motor behavior

Neuronal excitability is controlled by two broad classes of ion channels: voltage-gated and ligand-gated. It is well established that voltage-gated channels are not only composed of pore-forming subunits but auxiliary subunits as well, which are not part of the pore, but control many important aspects of channel function, such as trafficking and gating (1, 2). In contrast, ligand-gated ion channels were thought to function independently of auxiliary subunits. The discovery of the tetraspanning membrane protein stargazin, also referred to as  $\gamma$ -2, which is mutated in the ataxic *stargazer* (*stg*) mouse, changed this view. Cerebellar granule neurons (CGNs), which express high levels of stargazin, were found to lack surface AMPA-type glutamate receptors (AMPA receptors) in the *stg* mouse (3, 4). Stargazin not only controls the trafficking of AMPARs, but also controls AMPAR gating (5–10), indicating that it satisfies all of the criteria of auxiliary subunits. Stargazin is a member of a family of proteins referred to as transmembrane AMPA regulatory proteins (TARPs) and consists of the following members: canonical type I TARPs ( $\gamma$ -2,  $\gamma$ -3,  $\gamma$ -4, and  $\gamma$ -8) and atypical type II TARPs ( $\gamma$ -5 and  $\gamma$ -7), which differ in their amino acid sequence and uniquely regulate AMPAR trafficking, gating, and neuropharmacology (7).

Of particular interest is TARP  $\gamma$ -7, which is expressed throughout the brain but exhibits high levels of expression, along with  $\gamma$ -2, in cerebellar Purkinje cells (PCs) (11–14). Deleting  $\gamma$ -2 on its own

causes a ~60% reduction in AMPAR-mediated synaptic currents in PCs (14, 15). Widespread genetic deletion of  $\gamma$ -7 in the brain was shown to have a negligible effect on climbing fiber (cf) responses in cerebellar PCs. However, deleting  $\gamma$ -7 together with  $\gamma$ -2 (i.e., double knockout; dKO) all but abolishes cf responses, indicating that  $\gamma$ -7 may have a role in mediating a component of excitatory synaptic transmission in PCs. In addition, these dKO mice exhibit an ataxic gait that was more severe than the  $\gamma$ -2 knockout (KO) alone, whereas the  $\gamma$ -7 KO exhibited no detectable behavioral deficits (14). Whether the behavioral deficits seen in the dKO could be specifically attributed to the loss of excitatory synaptic transmission in PCs remains unclear.

In addition, the possible role of TARP  $\gamma$ -7 in mediating features of excitatory synaptic transmission in other cell types in the cerebellar cortex is unresolved. On the basis of *in situ* hybridization and immunohistochemistry,  $\gamma$ -7 is expressed in other cerebellar neuronal cell types including stellate cells (SCs) and granule neurons (CGNs) (11, 12, 14). Biochemical and heterologous expression studies have shown that  $\gamma$ -7 is capable of binding to AMPARs and enhancing AMPAR trafficking and gating in *stg* CGNs, albeit less effectively than  $\gamma$ -2 (12, 16). Furthermore, it has been proposed that  $\gamma$ -7 specifically associates

## Significance

**AMPA-type glutamate receptors (AMPA receptors) are the primary means through which the CNS carries out rapid, excitatory postsynaptic signaling. Members of the transmembrane AMPA regulatory protein (TARP) family of AMPAR auxiliary proteins are essential for the localization and function of AMPARs. Yet TARP family members differ in the ways in which they regulate AMPAR function. Much is known about the function of “typical” TARPs such as  $\gamma$ -2, but little about “atypical” TARPs such as  $\gamma$ -7. Using the cerebellar cortex as a model system, in which well-defined neuronal cell types exhibit differential expression of both  $\gamma$ -2 and  $\gamma$ -7, we examined the relative roles of these two TARP family members in both excitatory synaptic transmission and motor behavior related to cerebellar function.**

Author contributions: M.Y., C.E.L.P., A.C.J., and R.A.N. designed research; M.Y., C.E.L.P., A.C.J., and M.C. performed research; M.Y., C.E.L.P., A.C.J., K.S., and K.S.-L. analyzed data; and M.Y., C.E.L.P., A.C.J., and R.A.N. wrote the paper.

The authors declare no conflict of interest.

<sup>1</sup>M.Y., C.E.L.P., and A.C.J. contributed equally to this work.

<sup>2</sup>Present address: National Institute of Neurological Disorders and Stroke, National Institutes of Health, Bethesda, MD 20892.

<sup>3</sup>Present address: Department of Physiology and Neurobiology, University of Connecticut, Storrs, CT 06269.

<sup>4</sup>To whom correspondence may be addressed. Email: nicoll@cmp.ucsf.edu or alexander.jackson@uconn.edu.

This article contains supporting information online at [www.pnas.org/lookup/suppl/doi:10.1073/pnas.1423670112/-DCSupplemental](http://www.pnas.org/lookup/suppl/doi:10.1073/pnas.1423670112/-DCSupplemental).

with extrasynaptic, but not synaptic, GluA2-lacking AMPARs in *stg* SCs (17). Furthermore, recent work in CGNs compared the effect of shRNA-mediated knockdown of  $\gamma$ -7 to the overexpression of  $\gamma$ -7 in *stg* CGNs. Remarkably both manipulations caused a large increase in AMPAR currents, but their subunit composition differed. With knockdown, the additional receptors contained GluA2, whereas with overexpression, the additional receptors lacked GluA2 (18). Overall, these results suggest an intriguing interplay between  $\gamma$ -7 and  $\gamma$ -2 among neuronal cell types in the cerebellar cortex that may exhibit cell-type specificity. However, the role for  $\gamma$ -7 in cell type-specific AMPAR regulation remains obscure.

In the present study, we use a germ-line  $\gamma$ -7 KO mouse to investigate the relative contribution of  $\gamma$ -2 and  $\gamma$ -7 to excitatory synaptic transmission in cerebellar PCs, SCs, and CGNs. We found little to no contribution of  $\gamma$ -7 to excitatory transmission in SCs or CGNs, evidenced by the absence of a defect above and beyond that seen in *stg* alone. We confirmed that deleting  $\gamma$ -7 alone has no effect on PC AMPAR responses, but  $\gamma$ -7 deletion on the *stg* background resulted in the near-abolishment of AMPAR-mediated responses, leaving a small kainate receptor-mediated component intact. We further investigated the behavioral consequences of selectively silencing all excitatory inputs onto PCs. To this end, we crossed  $\gamma$ -7 KO mice, which have no behavioral phenotype, with a mouse in which  $\gamma$ -2 had been selectively deleted in PCs. The PCs in this mouse lack fast excitatory synaptic transmission and the mice exhibited severe motor deficits, most consistent with cerebellar abnormalities. These data suggest that  $\gamma$ -7 in PCs may have a role in supporting excitatory synaptic transmission in the absence of  $\gamma$ -2.

## Results

**Climbing Fiber-to-Purkinje Cell Excitatory Transmission Is Severely Impaired in *stg*/ $\gamma$ -7 Double KO Mouse Relative to *stg* Alone.** We first addressed the role that TARP  $\gamma$ -7 plays, relative to TARP  $\gamma$ -2, in excitatory synaptic transmission in three distinct neuronal cell types in the cerebellar cortex: PCs, SCs, and CGNs in the germ-line  $\gamma$ -7 KO mouse, the *stg* mouse (19), which lacks TARP  $\gamma$ -2, and a *stg*/ $\gamma$ -7 dKO mouse. We generated a  $\gamma$ -7 KO line by replacing the  $\gamma$ -7 gene with LacZ-Neo cassette (Fig. S1). Western blot analysis confirmed that  $\gamma$ -7 protein was absent in  $\gamma$ -7 KO brain homogenate (Figs. S1C and S3). As reported (12), we detected two bands in WT mouse brain by using a  $\gamma$ -7-specific antibody. The main band was of the molecular mass (31 kDa) predicted from the  $\gamma$ -7 amino acid sequence (20), and the other was slightly larger, indicating a posttranslational modification such as phosphorylation or glycosylation. For the characterization of PCs, we prepared acute cerebellar slices and used the cf-mediated excitatory postsynaptic current (EPSC) as the primary metric for the strength of excitatory synaptic transmission. We found that cf-EPSCs in  $\gamma$ -7 KO mice were not significantly different from WT mice, but were reduced by ~60% in the *stg* mouse (WT,  $2.11 \pm 0.29$  nA,  $n = 8$ ;  $\gamma$ -7-KO,  $2.26 \pm 0.21$  nA,  $n = 10$ ; *stg*,  $0.90 \pm 0.1$  nA,  $n = 14$ ) (Fig. 1A and B) as reported (15) and consistent with results from the widespread conditional deletion of  $\gamma$ -2 or  $\gamma$ -7 (14). Deleting both  $\gamma$ -7 and  $\gamma$ -2 caused a 90% reduction in cf-EPSCs (dKO,  $0.21 \pm 0.02$  nA,  $n = 13$ ) (Fig. 1A and B), also consistent with the widespread conditional deletion of both  $\gamma$ -7 and  $\gamma$ -2 (14). Because the hallmark of cf-EPSCs is their large, all-or-none current, we confirmed that the small remaining currents seen in the dKO were, in fact, mediated by cfs by satisfying two criteria: first, the remaining current had to be all-or-none; and second, the response had to exhibit paired-pulse depression. Furthermore, we found that the remaining current in the dKO is resistant to the AMPAR selective antagonist GYKI 53655 (100  $\mu$ M) and is mediated by kainate receptors (KARs) (15, 21). Thus, in the dKO, cf-EPSCs are largely mediated by current through KARs. The amplitude of the cf-evoked, KAR-

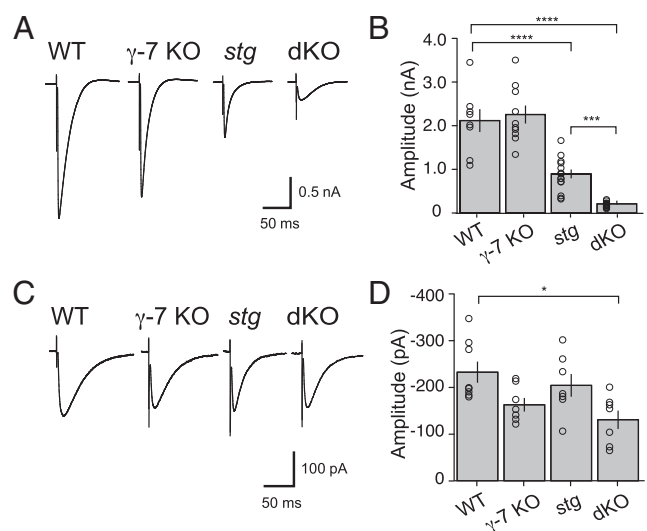


**Fig. 1.** AMPA receptor-mediated synaptic currents of Purkinje cells in *stg*/ $\gamma$ -7 double KO cerebella were significantly reduced. (A) Representative traces of climbing fiber-mediated EPSCs from WT,  $\gamma$ -7-KO, *stargazer* (*stg*), and *stg*/ $\gamma$ -7-KO (dKO). Climbing fibers (cfs) were stimulated in the granule cell layer at 0.1 Hz. Holding potential was  $-20$  mV. (B) Summary bar graph showing peak amplitudes of cf-EPSCs recorded from P31 to P58 mice. (C) Representative traces of kainate receptor (KAR)-mediated currents recorded in the presence of 100  $\mu$ M GYKI 53655 at  $-70$  mV. (D) Summary bar graph showing peak amplitudes of KAR-mediated cf-EPSCs. Bar graphs summarized average amplitudes  $\pm$  SEM. Open circles represent values from individual cells. Asterisks indicate significance, \* $P \leq 0.05$ , \*\*\* $P \leq 0.001$ , \*\*\*\* $P \leq 0.0001$ .

mediated current was similar among three genotypes (WT,  $232.46 \pm 25.23$  pA,  $n = 8$ ;  $\gamma$ -7-KO,  $163.11 \pm 14.6$  pA,  $n = 7$ ; *stg*,  $204.47 \pm 24.21$  pA,  $n = 7$ ) (Fig. 1C and D), suggesting that the number of cf synaptic contacts onto PCs was unaffected in these groups. However, KAR-mediated cf-EPSCs are decreased at dKO cf-PC synapses (dKO,  $131.02 \pm 19.57$  pA,  $n = 7$ ) (Fig. 1C and D), suggesting that excitatory input onto dKO PCs is reduced overall. Thus, *stg* PCs exhibit a significant reduction in synaptic AMPARs, with dKO PCs exhibiting a virtual abolishment of excitatory input.

### Excitatory Transmission in Cerebellar Stellate Cells Is Not Further Diminished in *stg*/ $\gamma$ -7 Double KO Mouse Relative to *stg* Alone.

We next examined the possible role that  $\gamma$ -7 may play in excitatory transmission in SCs, which express both  $\gamma$ -2 and  $\gamma$ -7 (11, 13). In the characterization of excitatory synaptic and extrasynaptic transmission in the *stg* mouse, AMPAR-mediated synaptic responses were found to be substantially diminished (17, 22). In our previous work, we showed that in the *stg* mouse, the average frequency of AMPAR-mediated miniature EPSCs (mEPSCs), arising from parallel fiber input from CGNs, was reduced by ~85% and the average amplitude by ~33% relative to WT (22). Using mEPSCs as the primary metric for excitatory input onto SCs, we asked whether the remaining synaptic AMPARs in *stg* SCs are accounted for by the presence of  $\gamma$ -7. Both the frequency and amplitude (Fig. 2A and C) of mEPSCs in dKO SCs were not significantly different from our previously published values from *stg* SCs (22), suggesting that  $\gamma$ -7 does not play a clear role in AMPAR trafficking in SCs, in the absence of  $\gamma$ -2. Furthermore, our previous data showed that extrasynaptic AMPARs are capable of cell-surface trafficking and are likely TARP-associated in *stg* SCs (22). Subsequent work confirmed that extrasynaptic AMPARs in *stg* SCs are TARP-associated and went on to show that they are specifically associated with  $\gamma$ -7 (17). We examined the possibility that  $\gamma$ -7 may be mediating the trafficking of extrasynaptic

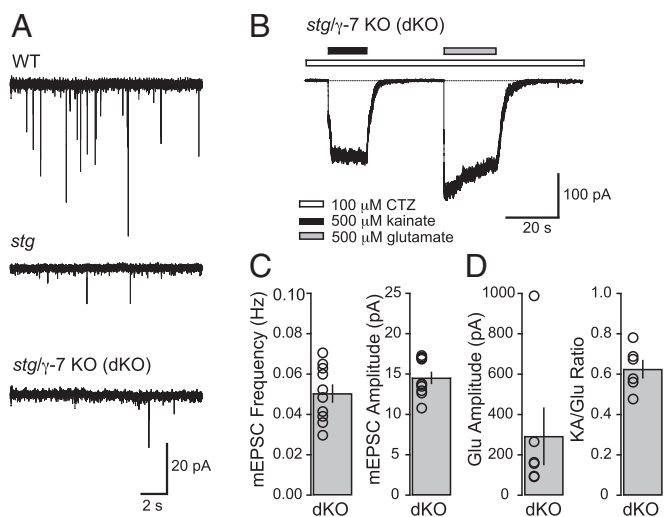


**Fig. 2.** Synaptic and extrasynaptic AMPARs in stellate cells from *stg/γ-7* double KO mice are not significantly reduced in comparison with *stargazer* mice alone. (A) Representative mEPSC traces (15 s long) from WT (Top), *stg* (Middle), and dKO (Bottom) cerebellar stellate cells (SCs) at a holding potential of  $-60$  mV. (B) Representative traces of currents evoked by  $500 \mu\text{M}$  kainate (black bars) and  $500 \mu\text{M}$  glutamate (gray bars) in a nucleated outside-out patch from a dKO SC soma at a holding potential of  $-60$  mV. Cyclothiazide (CTZ) is present in all solutions and is represented by a white bar. (C) Bar plots showing the average mEPSC frequency (Left) and amplitude (Right) of dKO SCs with individual values (open circles), represented as mean  $\pm$  SEM (mEPSC frequency,  $n = 10$ ; mEPSC amplitude,  $n = 10$ ). Neither frequency nor amplitude was significantly different from published values of *stg* SCs ( $P > 0.20$ ) (22). (D) Bar plot showing the average amplitude of glutamate-evoked currents (Left) and kainate/glutamate (KA/Glu) ratio (Right) from dKO SC nucleated patches with individual values (amplitude,  $n = 6$ ; KA/Glu ratio,  $n = 6$ ). Neither current amplitude nor KA/Glu ratio was significantly different from previously published values (22) of *stg* SCs ( $P > 0.10$ ).

AMPA receptors (AMPA) by recording from nucleated outside-out patches pulled from the somata of dKO SCs. We found that glutamate-evoked currents can be elicited from dKO nucleated patches with amplitudes that are not significantly different from published values of *stg* SCs (22) (Fig. 2B and D). Furthermore, the ratio between kainate (KA) and glutamate (Glu)-evoked currents (KA/Glu ratio), a metric for TARP association (10, 23), was not significantly different from published values from *stg* SCs (22) (Fig. 2B and D). These data suggest that, contrary to the predictions of recent studies, TARP  $\gamma-7$  does not appear to have a significant role to play in AMPAR function in cerebellar SCs.

**Excitatory Transmission in Cultured Cerebellar Granule Cells Is Unaffected by  $\gamma-7$  KO and Unchanged in *stg/γ-7* Double KO Mouse Relative to *stg* Alone.** We went on to examine CGNs, which express  $\gamma-7$ , in addition to  $\gamma-2$  (11, 12, 14). We examined the effect of deleting  $\gamma-7$  alone and in combination with the deletion of  $\gamma-2$  (*stg*) by using cultured CGNs. We found no significant difference in either the amplitude of spontaneous EPSCs (sEPSCs) or decay kinetics calculated from averaged waveforms in the  $\gamma-7$  KO mouse compared with WT (Fig. 3A and B). To control for other possible changes in excitatory synaptic transmission, we examined spontaneous NMDAR-mediated events (Fig. 3C) and whole-cell glutamate-evoked currents (Fig. 3D and E) and found no difference from WT. However, as reported (3), AMPAR-mediated sEPSCs were absent in *stg* CGNs (Fig. 3A), whereas NMDA sEPSCs remained intact (Fig. 3C). The whole-cell currents were also greatly reduced in *stg* CGNs (Fig. 3D and E). Examination of the dKO mouse demonstrates a phenotype indistinguishable from *stg* (Fig. 3). These results appear to differ substantially from previous results in which shRNA of  $\gamma-7$  in *stg* CGNs resulted in

a rescue of synaptic and whole-cell currents (17, 18). What might account for the difference? One possibility is the germ-line KO of  $\gamma-7$  may lead to a compensatory or developmental down-regulation of synaptic transmission. To address this possibility, we used the same shRNA constructs to knock down  $\gamma-7$  in cultured *stg* CGNs. In our hands, the fluorescence of the  $\gamma-7$ -shRNA-mCherry constructs reported (17, 18) was quite weak in CGNs. However, in *stg* CGNs expressing the shRNA-mCherry constructs, we failed to see any rescue of sEPSCs in contrast with previous reports. Concerned with the weak expression of this transfected construct, we used an alternative lentiviral expression approach, which strongly expressed the  $\gamma-7$ -shRNA-GFP constructs in the majority of CGNs (Fig. S2A). We recorded from a total of nine *stg* CGNs expressing shRNA-GFP and still failed to observe any rescue of sEPSCs (Fig. S2B). The shRNA target sequences we used were identical to those used in previous reports and were effective at greatly reducing the  $\gamma-7$  protein level in dissociated CGNs (Fig. S2C and D). Thus, we have no obvious explanation for the difference in our results compared with previous reports.

**Impaired Excitatory Transmission in a Purkinje Cell-Specific Conditional Deletion of  $\gamma-2$  With and Without a  $\gamma-7$  KO Background.** Widespread genetic deletion of both  $\gamma-2$  and  $\gamma-7$  in the brain has been shown to result in severe deficits in motor behavior, evident as ataxic gait (14). Given that germ-line deletion of  $\gamma-2$  (*stg*) and  $\gamma-7$  not only abolishes AMPAR-mediated synaptic transmission in PCs, but also severely impairs that of other cerebellar neurons and likely many other cell types throughout the CNS, it is not possible to identify the specific cellular defect that accounts for the motor deficits observed in the intact animal. We therefore investigated the electrophysiological and behavioral consequences of specifically deleting AMPAR-mediated transmission in PCs. We crossed the germ-line  $\gamma-7$  KO mouse, which has no obvious behavioral abnormalities (14), to a conditional  $\gamma-2$  KO mouse in which Cre recombinase is selectively expressed in PCs under the control of the L7 promoter (*Pcp2-cre*) (24). In this case, any physiological deficits should arise specifically from the synaptic impairments in the PCs lacking  $\gamma-2$ , with and without a germ-line  $\gamma-7$  KO background. This strategy would allow us to determine whether there are specific consequences of deleting  $\gamma-2$  only in PCs and if additional loss of  $\gamma-7$  reveals further deficits.

Here we define a simplified nomenclature for each of four genotype groups subsequently tested as follows: (i)  $\gamma-2$  PC WT:  $\gamma-7$  WT, mice with intact  $\gamma-2$  and  $\gamma-7$  expression whose genotype was  $L7\text{Cre}^-; \gamma-2^{\text{loxP/loxP}}; \gamma-7^{+/+}$ ; (ii)  $\gamma-2$  PC WT:  $\gamma-7$  KO, mice with intact  $\gamma-2$  expression and lacking  $\gamma-7$  whose genotype was  $L7\text{Cre}^-; \gamma-2^{\text{loxP/loxP}}; \gamma-7^{-/-}$  mice; (iii)  $\gamma-2$  PC KO:  $\gamma-7$  WT, mice with  $\gamma-2$  excised in PCs only, and intact  $\gamma-7$  expression, whose genotype was  $L7\text{Cre}^+; \gamma-2^{\text{loxP/loxP}}; \gamma-7^{+/+}$ ; and (iv)  $\gamma-2$  PC KO:  $\gamma-7$  KO, mice with  $\gamma-2$  excised in PCs only, and lacking  $\gamma-7$ , whose genotype was  $L7\text{Cre}^+; \gamma-2^{\text{loxP/loxP}}; \gamma-7^{-/-}$ .

To confirm the specificity of L7Cre recombinase activity to cerebellar Purkinje neurons, we crossed the L7Cre mouse to a ROSA26-tdTomato transgenic reporter mouse and found that tdTomato fluorescence in the 2-mo-old brain appeared to be confined to cerebellar Purkinje neuron dendrites and axons (Fig. 4A), consistent with the original description of the mouse (24). To evaluate the specificity of L7Cre-mediated recombination of the  $\gamma-2$  gene, we performed Western blot by using homogenates from each genotype group and confirmed that  $\gamma-2$  protein level in the forebrain was consistent between all groups, whereas cerebellar homogenates in both the  $\gamma-2$  PC KO;  $\gamma-7$  WT and  $\gamma-2$  PC KO;  $\gamma-7$  KO showed reduced  $\gamma-2$  protein levels compared with both L7Cre-negative control groups (Fig. S3). We then recorded cf-EPSCs from mice in each of the four groups (aged 3–4 mo). Cf responses were of normal size when recorded from either  $\gamma-2$  PC WT;  $\gamma-7$  WT ( $1.78 \pm 0.17$  nA;  $n = 9$ ) or  $\gamma-2$  PC

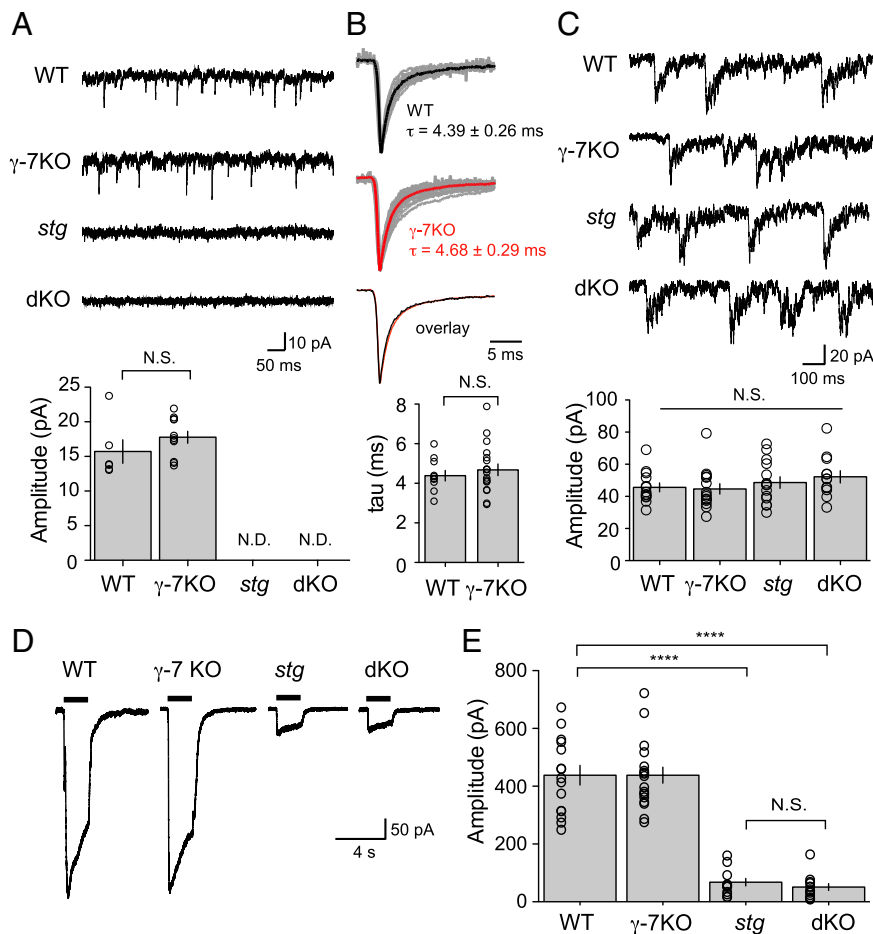


**Fig. 3.** TARP  $\gamma$ -7 has no apparent effect on AMPAR currents in dissociated cerebellar granule cells. (A) Spontaneous AMPA EPSCs recorded from WT,  $\gamma$ -7 KO, *stg*, and *stg*/ $\gamma$ -7 double mutant (dKO) cerebellar granule cells. Bar graph summarizes average amplitudes  $\pm$  SEM. WT,  $n = 6$ ;  $\gamma$ -7-KO,  $n = 11$ ; *stg*,  $n = 12$ ; dKO,  $n = 11$ . N.D., not detected. (B) Average miniature EPSCs from WT and  $\gamma$ -7 KO are normalized and aligned to the peak. Average mEPSC from individual neurons are displayed in gray, and averages of all experiments for both genotypes are shown in color. Weighted time constant values calculated from area under the peak-normalized current are displayed as mean  $\pm$  SEM. WT,  $n = 10$ ;  $\gamma$ -7-KO,  $n = 18$ . (C) Spontaneous NMDA EPSCs were normal in granule cells from all genotype. Bar graph summarized average amplitudes  $\pm$  SEM. WT,  $n = 13$ ;  $\gamma$ -7-KO,  $n = 15$ ; *stg*,  $n = 14$ ; dKO,  $n = 12$ . No significant difference was found among all genotype. (D) Typical current traces recorded from cerebellar granule cells in response to 1 mM glutamate plus 100  $\mu$ M CTZ and 100  $\mu$ M PEPA. Black bars represent the duration of agonist application. (E) Bar graph summarizes average amplitudes  $\pm$  SEM. WT,  $n = 15$ ;  $\gamma$ -7-KO,  $n = 18$ ; *stg*,  $n = 12$ ; dKO,  $n = 13$ . \*\*\*\* $P \leq 0.0001$ . N.S., not significant. Open circles represent values from individual cells.

WT;  $\gamma$ -7 KO mice ( $1.86 \pm 0.18$  nA;  $n = 8$ ) (Fig. 4 B and C). However, in  $\gamma$ -2 PC KO;  $\gamma$ -7 WT mice, the amplitude of cf-PC EPSCs was halved ( $1.05 \pm 0.13$  nA;  $n = 9$ ) compared with control groups. This observation is consistent with the recent report of Kawata et al (25). Moreover, in  $\gamma$ -2 PC KO;  $\gamma$ -7 KO mice, the cf responses were greatly diminished ( $0.22 \pm 0.03$  nA;  $n = 14$ ) (Fig. 4 B and C) similar to those recorded in the global  $\gamma$ -2 and  $\gamma$ -7 dKO (14) and *stg*/ $\gamma$ -7 dKO (Fig. 1A).

Interestingly, the deficits in PC-specific conditional KO mice ( $\gamma$ -2 PC KO;  $\gamma$ -7 WT and  $\gamma$ -2 PC KO;  $\gamma$ -7 KO mice) were not as dramatic in younger animals [postnatal day (P)17–P24] (Fig. S4 B and D), suggesting the phenotype may take some time to develop because of a delay in cre recombinase expression in the L7Cre mouse (24), or another TARP may be expressed in early postnatal developmental stages to maintain normal synapse activity. However, a strong reduction of the cf-PC synaptic response was seen in the global  $\gamma$ -2 and  $\gamma$ -7 dKO through early developmental stages (Fig. S4 A and C). This result suggests that  $\gamma$ -2 and  $\gamma$ -7 are expressed at an early developmental stage and are essential for cf-PC EPSCs. Although PCs in the  $\gamma$ -2 PC KO;  $\gamma$ -7 WT exhibit impaired synaptic transmission, and  $\gamma$ -2 PC KO;  $\gamma$ -7 KO PCs are essentially devoid of excitatory synaptic trans-

mission, we did not detect a difference in overall cerebellar size and any overt abnormalities in the lamination or foliation of each cerebellum (up to 4 mo old). Instead, the KAR-mediated responses, which were resistant to 100  $\mu$ M GYKI 53655, were enhanced in  $\gamma$ -2 PC KO;  $\gamma$ -7 KO PCs (Fig. 4 D and E). This enhancement was not observed in global *stg*/ $\gamma$ -7 dKO (Fig. 1D). These results suggest that the potentiation of KAR channels may represent a homeostatic mechanism (26) to maintain synaptic activity and anatomical structure in  $\gamma$ -2 PC KO;  $\gamma$ -7 KO PCs.

**Impaired Motor Behavior in a Purkinje Cell-Specific Conditional Deletion of  $\gamma$ -2 with a  $\gamma$ -7 KO Background.** We next carried out a battery of behavioral tests to provide a detailed characterization of any motor deficits exhibited by the Purkinje cell-specific deletion of  $\gamma$ -2 with and without a  $\gamma$ -7 KO background. The four previously defined genotype groups were tested (Fig. 4). Each genotype group was comprised of a mixture of males and females aged between 5 and 12 mo (see further details in Table S1).

The first test was a simple observational score of whether each mouse displayed an ataxic gait. The  $\gamma$ -2 PC KO;  $\gamma$ -7 KO mice were all ataxic, whereas none of the mice from the other three groups displayed ataxia (Table S2). The ataxic mice could move

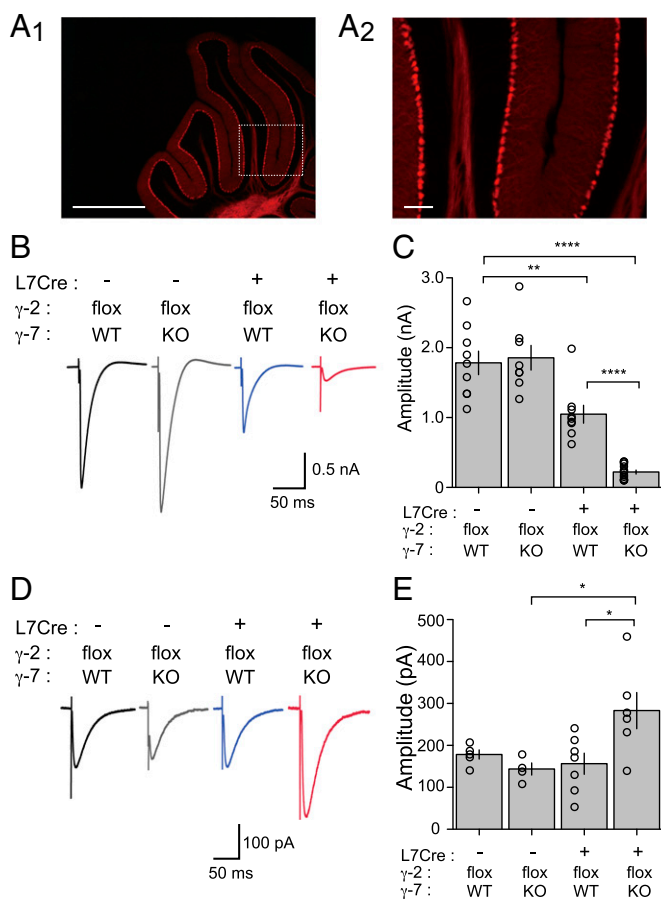


**Fig. 4.** AMPA receptor-mediated synaptic currents were significantly reduced in Purkinje cell-specific  $\gamma$ -2/ $\gamma$ -7 double KO mice. (A) Fluorescent micrograph of cerebellum prepared from L7Cre; ROSA26-tdTomato mice. L7Cre mouse was crossed with ROSA26-tdTomato reporter line and analyzed at 2 mo old. White box in *Left* indicates brain region shown in *Right*. (Scale bars: *Left*, 1 mm; *Right*, 100  $\mu$ m.) (B) Representative traces of cf-EPSCs recorded from  $\gamma$ -2 PC WT;  $\gamma$ -7 WT (L7Cre<sup>-</sup>;  $\gamma$ -2<sup>flox</sup>;  $\gamma$ -7 WT, black),  $\gamma$ -2 PC WT;  $\gamma$ -7 KO (L7Cre<sup>-</sup>;  $\gamma$ -2<sup>flox</sup>;  $\gamma$ -7 KO, gray),  $\gamma$ -2 PC KO;  $\gamma$ -7 WT (L7Cre<sup>+</sup>;  $\gamma$ -2<sup>flox</sup>;  $\gamma$ -7 WT, blue), and  $\gamma$ -2 PC KO;  $\gamma$ -7 KO (L7Cre<sup>+</sup>;  $\gamma$ -2<sup>flox</sup>;  $\gamma$ -7 KO, red) mice. (C) Summary bar graph showing peak amplitudes of cf-EPSCs recorded from P63 to 4-mo-old mice at the holding potential of  $-20$  mV. (D) Representative traces of KAR-mediated currents recorded from  $\gamma$ -2 PC WT;  $\gamma$ -7 WT (black),  $\gamma$ -2 PC WT;  $\gamma$ -7 KO (gray),  $\gamma$ -2 PC KO;  $\gamma$ -7 WT (blue), and  $\gamma$ -2 PC KO;  $\gamma$ -7 KO (red) mice in the presence of 100  $\mu$ M GYKI 53655 at  $-70$  mV. (E) Summary bar graph showing the KAR EPSCs. Open circles represent values from individual cells. Asterisks indicate significance, \* $P \leq 0.05$ , \*\* $P \leq 0.01$ , \*\*\*\* $P \leq 0.0001$ .

around, but their gait was shaky and their stride was shorter, evident in footprint patterns (Fig. 5D compared with Fig. 5A–C). Examples of the ataxia can be observed in [Movies S1](#) and [S2](#). Body weights of the  $\gamma$ -2 PC KO;  $\gamma$ -7 KO mice were within a healthy range and were statistically no different from the other genotype groups (Fig. S5A). The abnormal locomotion of these mice was obviously noticeable at 3 mo of age, with a progressive worsening of the ataxic gait with further aging (e.g., 5 mo vs. 3 mo; Fig. 5). Perhaps unexpectedly, mice lacking only  $\gamma$ -2 in PCs ( $\gamma$ -2 PC-KO;  $\gamma$ -7 WT) had an apparently normal gait, at least by this simple qualitative scoring (Fig. 5C).

Next, mice were trained on the rotarod (Fig. 6B). When the genotypes were unblinded, all of the  $\gamma$ -2 PC KO;  $\gamma$ -7 KO mice had been excluded from the training sessions because of severe impairment and one  $\gamma$ -2 PC WT;  $\gamma$ -7 KO mouse that was obese (50.3 g at time of training). Taking into account only the first

session trials (S1T1–S1T4), a repeated measures two-way ANOVA with  $\gamma$ -2 PC and  $\gamma$ -7 genotypes as factors showed a significant main effect of the  $\gamma$ -2 PC genotype only ( $P = 0.0057$ ). Pairwise comparisons for individual trials showed significant differences between  $\gamma$ -2 PC KO;  $\gamma$ -7 KO mice (red) and both  $\gamma$ -2 PC WT;  $\gamma$ -7 KO (gray) as well as  $\gamma$ -2 PC WT;  $\gamma$ -7 WT (black) mice for S1T2, S1T3, and S1T4 (Fig. 6B; \* $P \leq 0.0166$ , Student's *t* test). Comparing the three genotype groups that could successfully be trained across all trials, in a repeated measures two-way ANOVA, there was no significant difference between groups. However, in sessions 1 and 2, there was a trend that  $\gamma$ -2 PC KO;  $\gamma$ -7 WT mice (blue), lacking  $\gamma$ -2 in PCs but with intact  $\gamma$ -7, were slower to learn the task. They caught up to the performance level of  $\gamma$ -2 PC WT mice by the third training session (S3T1–S3T4). Furthermore, there were no differences among these three groups in the final rotarod assessment that followed the training sessions (Fig. S5B). The complete inability of  $\gamma$ -2 PC KO;  $\gamma$ -7 KO mice to learn to walk on the rotarod indicates a motor deficit most consistent with cerebellar dysfunction.

In the open field, both for total ambulation (Fig. 6C) and rearing behavior (Fig. 6D), two-way ANOVA analysis showed significant main effects of both the  $\gamma$ -2 PC genotype ( $P \leq 0.0181$ ) and the  $\gamma$ -7 genotype ( $P \leq 0.0087$ ), as well as an interaction between the two ( $P \leq 0.0233$ ). Post hoc comparisons showed that  $\gamma$ -2 PC KO;  $\gamma$ -7 KO mice ambulated significantly less than the three other groups for the first two trials (Fig. 6C; \* $P < 0.0001$ , Student's *t* test pairwise comparisons) and also reared less during these trials (Fig. 6D; \* $P \leq 0.002$ , Student's *t* test pairwise comparisons). By the third trial, because all mice habituate to the open field chamber, the differences were less pronounced, although the  $\gamma$ -2 PC KO;  $\gamma$ -7 KO mice were still significantly different from the  $\gamma$ -2 PC WT;  $\gamma$ -7 WT and  $\gamma$ -2 PC WT;  $\gamma$ -7 KO mice for both ambulation (Fig. 6C, #) and rears (Fig. 6D, #). Interestingly, in the first and third trials, the  $\gamma$ -2 PC WT;  $\gamma$ -7 WT mice (black) ambulated significantly more than the  $\gamma$ -2 PC WT;  $\gamma$ -7 KO mice (gray) (Fig. 5C, ^). However, this effect was driven in part by obese mice (>35 g) in the  $\gamma$ -2 PC WT;  $\gamma$ -7 KO group (gray; when excluded, the significance for OF3 disappears, and the significance for OF1 is greatly diminished, from  $P = 0.0061$  to  $P = 0.0385$ ), and furthermore, there were no other differences between these two groups. Overall, the open field data showed that mice on the  $\gamma$ -7 KO background, also lacking  $\gamma$ -2 in PCs, locomoted less overall and were less able to rear up on their hind legs to explore the chamber.

The wire hang test is an assessment of neuromuscular function and motor coordination. Two-way ANOVA analysis revealed a significant main effect of the  $\gamma$ -2 PC genotype ( $P < 0.0001$ ) and also the  $\gamma$ -7 genotype ( $P = 0.0104$ ), but no interaction between the two. In this test as well,  $\gamma$ -2 PC KO;  $\gamma$ -7 KO mice were significantly impaired compared with the other three genotype groups because they were only able to hang for an average of 10 s, whereas the other groups could remain hanging for at least an average of 34 s (Fig. 6E;  $P \leq 0.0056$ , Student's *t* test pairwise comparisons). There is a known body weight confound to this test, in that overweight mice will tend to perform more poorly. Wire hang latency plotted versus body weight (Fig. 6F) shows that several of the mice (e.g., >35 g) were likely impaired because of body weight rather than a true motor defect. Of note, the great majority of  $\gamma$ -2 PC KO;  $\gamma$ -7 KO mice were under 30 g in body weight and, thus, their deficits in this test were not attributable to high body weight but rather to a functional consequence of lacking both  $\gamma$ -2 and  $\gamma$ -7 in PCs.

Finally, all mice were assessed for both forelimb and hindlimb grip strength (Fig. 6G and H). Here again, by two-way ANOVA, there were significant main effects of both the  $\gamma$ -2 PC genotype ( $P < 0.0001$  for forelimb;  $P = 0.0046$  for hindlimb) and the  $\gamma$ -7 genotype ( $P = 0.0237$  for forelimb;  $P = 0.0112$  for hindlimb) as well as an interaction between the two ( $P = 0.0011$  for forelimb;

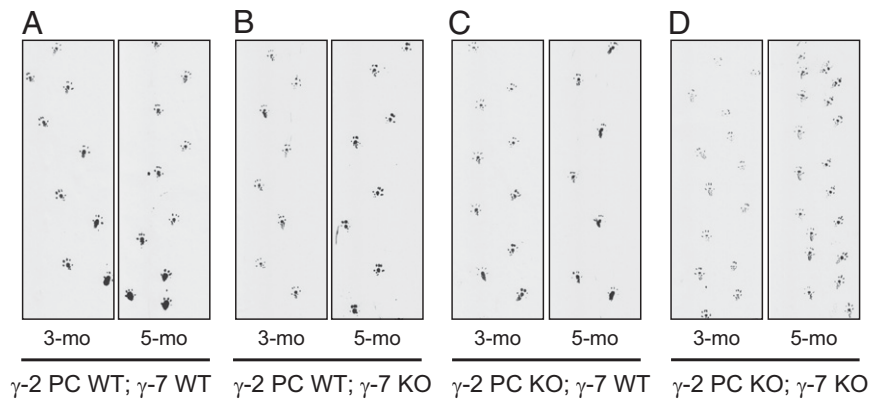


**Fig. 5.** Abnormal gait was observed in  $\gamma$ -2 PC KO;  $\gamma$ -7 KO mice. Examples of footprint patterns from  $\gamma$ -2 PC WT;  $\gamma$ -7 WT (A),  $\gamma$ -2 PC WT;  $\gamma$ -7 KO (B),  $\gamma$ -2 PC KO;  $\gamma$ -7 WT (C), and  $\gamma$ -2 PC KO;  $\gamma$ -7 KO (D) mice at 3 (3-mo) and 5 (5-mo) month old are shown.  $\gamma$ -2 PC KO;  $\gamma$ -7 KO mouse showed the most severely ataxic gait. Their steps appear to be progressively shorter than other genotypes.

$P = 0.0138$  for hindlimb). Individual pairwise comparisons showed that  $\gamma$ -2 PC KO;  $\gamma$ -7 KO mice were significantly different from all other genotype groups, with weaker force measurements for both forelimbs ( $P \leq 0.0006$ ) and hindlimbs ( $P \leq 0.0024$ ) (Fig. 6 G and H; \*, Student's  $t$  test), indicating that the lack of both  $\gamma$ -2 and  $\gamma$ -7 in PCs cells is relevant to the ability to coordinate a strong grip.

In summary, all behaviors tested in the four genotype groups revealed motor impairments in the  $\gamma$ -2 PC KO;  $\gamma$ -7 KO mice, whereas the  $\gamma$ -2 PC KO;  $\gamma$ -7 WT mice were comparable to  $\gamma$ -2 PC WT;  $\gamma$ -7 WT and  $\gamma$ -2 PC WT;  $\gamma$ -7 KO mice. As noted, germline  $\gamma$ -7 knockouts appeared no different from WT mice (14). Overall, these data suggest that at the level of behavioral output,  $\gamma$ -7 can compensate for the loss of  $\gamma$ -2 in PCs, whereas the loss of both subunits has extremely severe consequences on motor function.

## Discussion

Members of the TARP family of AMPAR auxiliary subunits play critical roles in the function of all known excitatory synapses in the cerebellum. TARP  $\gamma$ -2, which is expressed in all neuronal types in the cerebellum, has been shown to determine the number of synaptic AMPARs at mossy fiber-to-CGN synapses (3, 4, 14), parallel fiber-to-PC synapses and climbing fiber-to-PC synapses (14, 15), parallel fiber-to-SC synapses (17, 22), and parallel fiber-to-Golgi cell synapses (15). Less clear is the role of the type II TARP  $\gamma$ -7, which is expressed, along with  $\gamma$ -2 and often other TARP family members, in CGNs, PCs, and SCs (11, 16). In this study, we undertook an examination of the specific roles that this TARP family member may play in excitatory synaptic transmission among these cerebellar cell types and their role in motor behavior. Using the *stg* mouse, our germ-line  $\gamma$ -7 KO mouse, and a *stg*/ $\gamma$ -7 dKO mouse, we failed to detect any clear contribution of  $\gamma$ -7 to excitatory transmission in SCs or CGNs but did observe a contribution of  $\gamma$ -7 to cf input onto PCs, suggesting a unique role for  $\gamma$ -7 in regulating synaptic transmission in PCs. At the behavioral level, we found that  $\gamma$ -7 in PCs may be capable of maintaining essentially normal motor behavior in the absence of  $\gamma$ -2, thus revealing a role for  $\gamma$ -7 in cerebellar PC-dependent motor behavior.

In principle,  $\gamma$ -7 seems well-positioned to contribute to AMPAR trafficking and gating in multiple neuronal cell types in the cerebellum, where it is enriched relative to other brain regions (12). TARP  $\gamma$ -7 is expressed ubiquitously in the cerebellum, from the abundant CGNs to cerebellar interneurons (such as SCs) and in the only output neurons of the cerebellum, the PCs (11, 12, 14). In addition, recent work suggests that  $\gamma$ -7 has specialized roles to

play in compartment- and subunit-specific AMPAR trafficking in SCs and CGNs (17, 18).

With regard to cerebellar SCs, we examined the possibility that  $\gamma$ -7 may account for the remaining AMPAR-mediated transmission left at both parallel fiber-to-SC excitatory synapses and at extrasynaptic sites in the absence of  $\gamma$ -2 (17, 22). In particular, the amplitude of glutamate-evoked currents from nucleated outside-out patches is unchanged in *stg* SCs relative to WT (22), and several lines of evidence suggest that these extrasynaptic/somatic AMPARs are in fact TARP-associated (17, 22). Bats et al. (17) confirmed that extrasynaptic AMPARs in *stg* SCs are TARP-associated and suggested that they are specifically associated with  $\gamma$ -7. They went on to use cultured granule cells as a proxy for a population of  $\gamma$ -2/ $\gamma$ -7-expressing neurons, knocked down  $\gamma$ -7 in *stg* cultures by using an shRNA approach and paradoxically found that AMPAR-mediated mEPSCs are robustly rescued. Their interpretation is that  $\gamma$ -7 somehow impedes the synaptic targeting of TARPlless AMPARs to synapses in the absence of  $\gamma$ -2 (17). Based on these data, a prediction would be that *stg* SCs, with a  $\gamma$ -7 KO background, would exhibit an enhancement in synaptic AMPARs (if  $\gamma$ -7 indeed interrupts synaptic targeting of TARPlless AMPARs) and an abolishment of extrasynaptic AMPARs (if  $\gamma$ -7 is indeed mediating trafficking to extrasynaptic sites). Surprisingly, our recordings fulfill neither of these predictions: mEPSCs from *stg*/ $\gamma$ -7 dKO mice are not significantly different from *stg* and extrasynaptic AMPARs are largely preserved. Furthermore, the KA/Glu ratio is unaffected, suggesting that extrasynaptic AMPARs in *stg*/ $\gamma$ -7 dKO mice are unlikely to be TARPlless. These data would suggest, contrary to the predictions of previous work, that  $\gamma$ -7 is unlikely to play a significant role in either synaptic or extrasynaptic AMPAR function in cerebellar SCs.

In  $\gamma$ -7 germ-line KO mice, we were unable to detect any impairment in either surface or synaptic AMPAR function in CGNs and the *stg*/ $\gamma$ -7 dKO phenotype was indistinguishable from *stg*. These data are in contrast to recent work showing that shRNA knockdown of  $\gamma$ -7 caused dramatic changes in synaptic and extrasynaptic AMPAR responses of CGNs (17, 18). One possibility is that the effect of acutely removing  $\gamma$ -7 differs from germ-line deletion, which may lead to developmental changes or compensation. We addressed this possibility by using the identical shRNA construct used in the previous studies and found no effect of knocking down  $\gamma$ -7. To address the possibility that the knockdown was inadequate in CGNs, we turned to a lentiviral system for the shRNA expression. This construct was expressed in the large majority of CGNs and severely reduced the expression of  $\gamma$ -7 protein (Fig. S2).

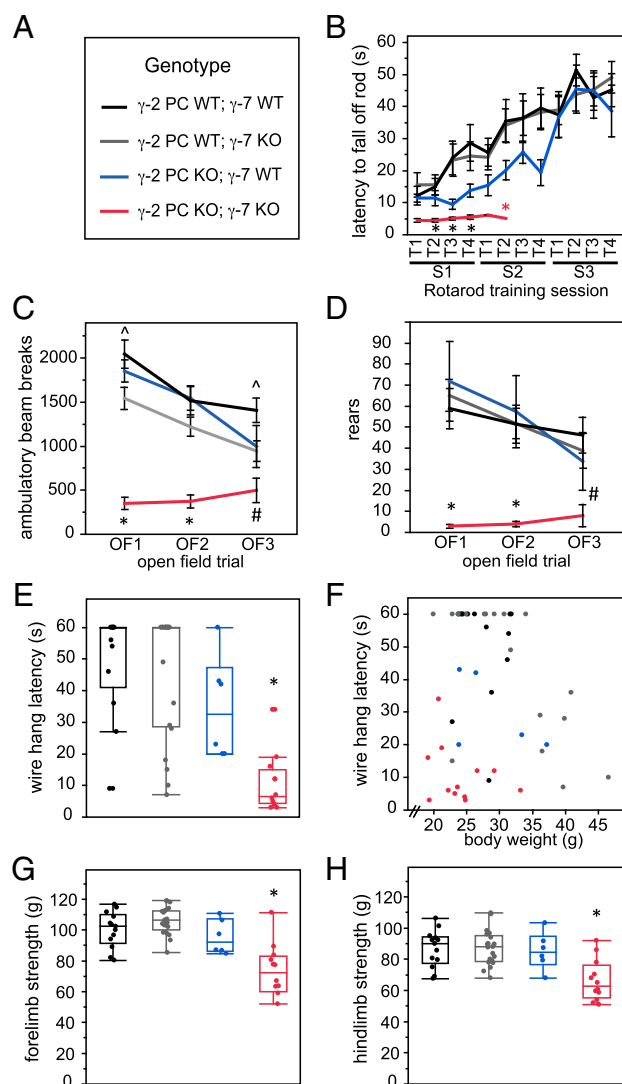


**Fig. 6.** Motor behaviors are impaired in  $\gamma$ -7 KO mice also lacking  $\gamma$ -2 in Purkinje cells. (A) Genotype legend. Black,  $\gamma$ -2 PC WT;  $\gamma$ -7 WT. Gray,  $\gamma$ -2 PC WT;  $\gamma$ -7 KO. Blue,  $\gamma$ -2 PC KO;  $\gamma$ -7 WT. Red,  $\gamma$ -2 PC KO;  $\gamma$ -7 KO. Data represented in B–D are mean  $\pm$  SEM. (B) Rotarod training.  $\gamma$ -2 PC KO;  $\gamma$ -7 KO mice (red) performed significantly worse than  $\gamma$ -2 PC WT;  $\gamma$ -7 WT (black) and  $\gamma$ -2 PC WT;  $\gamma$ -7 KO (gray) controls. Red asterisk denotes that training sessions were discontinued for  $\gamma$ -2 PC KO;  $\gamma$ -7 KO mice (red) because they could not learn the task. Significant differences in pairwise comparisons for individual trials: in S1T2,  $*P = 0.0169$  for red vs. black, and  $P = 0.0086$  for red vs. gray; in S1T3,  $*P = 0.0112$  for red vs. black, and  $P = 0.0107$  for red vs. gray; in S1T4  $*P = 0.0016$  for red vs. black, and  $P = 0.0063$  for red vs. gray. (C) Open field total horizontal ambulation during three trials OF1, OF2, and OF3.  $\gamma$ -2 PC KO;  $\gamma$ -7 KO mice (red) locomoted significantly less than mice from control groups. Individual pairwise comparisons:  $*P < 0.0001$ ,  $\gamma$ -2 PC KO;  $\gamma$ -7 KO mice (red) moved less than all three control groups for OF1 and OF2;  $\#P \leq 0.0235$ , red vs. black and gray in OF3;  $\wedge P \leq 0.0166$ , black vs. gray in OF1 and OF3. (D) Open field rearing behavior during three trials OF1, OF2, and OF3.  $\gamma$ -2 PC KO;  $\gamma$ -7 KO mice (red) reared significantly less than mice from control groups. Individual pairwise comparisons:  $*$ ,  $\gamma$ -2 PC KO;  $\gamma$ -7 KO mice (red) significantly different from all three control groups,  $P \leq 0.0001$  (OF1),  $P \leq 0.002$  (OF2);  $\#P \leq 0.0111$ , red vs. black and gray (OF3). (E) Maximum latency (best of three trials) in the wire hang test.  $\gamma$ -2 PC KO;  $\gamma$ -7 KO mice (red) were significantly impaired compared with all control groups: vs. black and gray,  $P < 0.0001$ ; vs. blue,  $P = 0.0056$ .  $*$ , at least  $P \leq 0.0056$ . (F) Maximum wire hang latency data (as shown in E) plotted versus body weight, showing that some mice that could not perform the task properly were overweight (e.g.,  $>35$  g). (G) Average of three measurements of forelimb strength.  $\gamma$ -2 PC KO;  $\gamma$ -7 KO mice (red) were significantly impaired compared with all other control groups. Pairwise comparisons:  $*P \leq 0.0006$  ( $P < 0.0001$  for red vs. both black and

gray;  $P = 0.0006$  for red vs. blue). (H) Average of three measurements of hindlimb strength.  $\gamma$ -2 PC KO;  $\gamma$ -7 KO mice (red) were significantly impaired compared with all other control groups. Pairwise comparisons:  $*P \leq 0.0024$  ( $P < 0.0001$  for red vs. black and gray;  $P = 0.0024$  for red vs. blue). All  $P$  values for pairwise comparisons calculated with a two-way Student's  $t$  test.

Again, we could find no effect of knocking down  $\gamma$ -7 in CGNs. In conclusion, our results suggest that  $\gamma$ -7 does not play a role in either synaptic or extrasynaptic AMPAR function in SCs and CGNs. We have no clear explanation for the difference between our results and previous results (17, 18). However, in agreement with previous results (14), we found that deletion of both TARPs  $\gamma$ -2 and  $\gamma$ -7 in PCs resulted in almost complete loss of cf-mediated AMPA EPSCs (Fig. 1), indicating a critical role for  $\gamma$ -7 in PCs. Cerebellar PCs are the sole output neurons of the cerebellar cortex and project to the deep cerebellar nuclei and vestibular nuclei neurons, which are involved in motor control in animals through their communication with the nuclei of the thalamus and brainstem (27). In *stg* mutant mice,  $\gamma$ -2 gene expression is disrupted at the genomic level and excitatory transmission is affected to varying degrees at all excitatory synapses in the cerebellum (and anywhere in brain where  $\gamma$ -2 is expressed), presumably accounting for the ataxic phenotype. To limit the phenotype to PCs, we crossed a  $\gamma$ -2-floxed mouse with an *L7Cre* mouse resulting in the  $\gamma$ -2 gene being specifically knocked out in PCs ( $\gamma$ -2 PC KO). These mice were, in turn, bred with ( $\gamma$ -2 PC KO;  $\gamma$ -7 KO) and without ( $\gamma$ -2 PC KO;  $\gamma$ -7 WT) the germ-line  $\gamma$ -7 KO background, which alone exhibited no clear electrophysiological or behavioral phenotype. We showed that cf-EPSCs were essentially abolished in  $\gamma$ -2 PC KO;  $\gamma$ -7 KO mice after 3 mo of age, whereas those in  $\gamma$ -2 PC KO;  $\gamma$ -7 WT mice remained with only half the amplitude of control cf-EPSCs (Fig. 4 B and C). Recently, it has been reported that the late phase of cf elimination was impaired in PC-selective  $\gamma$ -2 KO mice, with the absolute strengths of cf inputs scaled down and cf-induced  $\text{Ca}^{2+}$  transients significantly reduced (25). Because excitatory synaptic transmission to PCs is primarily mediated by AMPARs after the third postnatal week (28, 29), the smaller amplitude of AMPAR-mediated EPSCs, and reduced activation of P/Q-type voltage-dependent calcium channels, resulted in multiple cf innervation of PCs (25). We have not examined whether synapse elimination is impaired in our  $\gamma$ -2 PC KO mutant, but this recent data suggest that our  $\gamma$ -2 PC KO;  $\gamma$ -7 WT and  $\gamma$ -2 PC KO;  $\gamma$ -7 KO mutants likely exhibit multiple cf innervation, although we included responses in our study that were all or none. It would be of considerable interest to examine both multiple climbing fiber innervation and changes in intrinsic excitability in the  $\gamma$ -2 PC KO;  $\gamma$ -7 WT and  $\gamma$ -2 PC KO;  $\gamma$ -7 KO mutants generated in the current study. In addition, it would be of interest to determine the mechanism underlying the role of TARPs in the apparent age-dependent decline in motor function (Fig. 5 and Fig. S4) and the possibility of late-stage cerebellar dysfunction or degeneration. Finally, we found that KA receptor-mediated responses were enhanced in  $\gamma$ -2 PC KO;  $\gamma$ -7 KO mice (Fig. 4 D and E). Because global *stg*/ $\gamma$ -7 dKO mice did not exhibit such enhancement, rather a decrease relative to WT (Fig. 1 C and D), it is possible that this enhancement reflects a homeostatic effect of the late-onset loss of cf-EPSC responses as a way of maintaining synaptic activity, previously reported in *stg* CGNs (26). However,  $\gamma$ -2 PC KO;  $\gamma$ -7 WT mice showed no reduction in KA responses, indicating that approximately half of control levels of excitatory cf input onto PCs is sufficient to maintain essentially normal cerebellar function.

The battery of motor tests performed points to several consistent results: (i) the  $\gamma$ -2 PC WT;  $\gamma$ -7 KO mouse group is no different from the wild type group ( $\gamma$ -2 PC WT;  $\gamma$ -7 WT), corroborating

previous findings that global deletion of  $\gamma$ -7 has no observable phenotype (14); (ii) the  $\gamma$ -2 PC KO;  $\gamma$ -7 WT mouse group is, for the most part, unimpaired despite an ~50% reduction in excitatory synaptic input onto PCs, although it may exhibit slower learning in the rotarod, and (iii)  $\gamma$ -2 PC KO;  $\gamma$ -7 KO mice are severely impaired, therefore the combinatorial deletion of  $\gamma$ -2 and  $\gamma$ -7 in PCs has dramatic and deleterious consequences on motor behavior. The wide-ranging motor deficits detected in these mice include ataxic gait, severely reduced ambulation and rearing in the open field, impaired performance in the wire hang test, and reduced forelimb and hindlimb grip strength. The battery of tests is more confirmatory than any single stand-alone test, and the consistency of results between the different tests gives us more confidence that the observed effects are real and robust.

These data suggest that both  $\gamma$ -2 and  $\gamma$ -7 TARP subunits have a role to play in excitatory transmission in PCs in contrast to the other cerebellar cell types that we studied. In PCs, the loss of  $\gamma$ -7 can clearly be compensated for by  $\gamma$ -2 and, most interestingly, the loss of  $\gamma$ -2 can largely be compensated for by  $\gamma$ -7, despite a dramatic loss in excitatory transmission, to maintain essentially normal cerebellar function and motor coordination. It has been reported that  $\gamma$ -7 is enriched in the postsynaptic density (PSD) (12, 14) and associated with PSD-95, although it lacks a typical PDZ binding motif on its C-tail (12). Our results suggested that  $\gamma$ -7 presumably interacts with PSD proteins, and the maintenance of intact cf fiber input through multiple mechanisms may represent an important compensatory strategy for preserving a key instructive signal in motor learning (30, 31). Together, our results show that  $\gamma$ -2 and  $\gamma$ -7 TARP subunits are required for AMPAR-mediated cf input onto PCs and that this excitatory input is necessary for the proper control of motor function and coordination involved in the behaviors examined. Although there are multiple prior examples of global deletions causing cerebellar synaptic abnormalities and impaired motor coordination (32–35), to our knowledge, this is the first example of abolishment of excitatory input specifically onto Purkinje cells, which provides us with additional insight into the relationship between Purkinje cell function and control of motor coordination.

## Materials and Methods

**Animals.** All experiments were carried out in accordance with animal welfare regulations set out by the University of California, San Francisco Institutional Animal Care and Use Committee. Protocols for mouse behavior experiments were approved by the Genentech Animal Care and Use Committee, and these

experiments were conducted at Genentech according to NIH guidelines for the humane care and treatment of laboratory animals. *Stargazer* mutant mice and TARP  $\gamma$ -2-floxed mice (14) have been described. TARP  $\gamma$ -7 KO mice were generated by Deltagen (see *SI Materials and Methods*). *Stargazer* mice were bred to  $\gamma$ -7 KO mice to generate homozygous  $\gamma$ -7KO/*stargazer* double KO mice. WT mice were acquired from WT breeding pairs derived from the *stargazer* background. L7-Cre mice (stock no. 010536; B6.Cg-Tg(Pcp2-cre)3555<sup>Jdhuj</sup>; The Jackson Laboratory) (24) were used for cerebellar Purkinje cell-specific deletion of floxed TARP  $\gamma$ -2 gene. ROSA26-tdTomato reporter line (stock no. 007909; B6.Cg-Gt(ROSA)26Sor<sup>tm9(CAG-tdTomato)HzeJJ</sup>; The Allen Institute for Brain Science and The Jackson Laboratory) (36) was used for characterization of Cre-mediated recombination.

**Brain Slice Preparation and Electrophysiology.** Mice were anesthetized with isoflurane, decapitated, and their brains were rapidly removed and placed in an ice-cold, high-sucrose cutting solution. Parasagittal cerebellar slices (250  $\mu$ m thick) and transverse cerebellar slices (250  $\mu$ m thick) were prepared, and whole-cell recordings from visually identified Purkinje cells and stellate cells were obtained at room temperature (21–22 °C). Compositions of the external and internal solution, and protocols of recording, are described in *SI Materials and Methods*.

**Dissociated Cerebellar Granule Neuron Culture and Electrophysiology.** The dissociation and culture of cerebellar granule neurons were performed following the protocol provided in previous work (12, 37). Whole-cell patch-clamp recordings were made 8–10 d in vitro (DIV) as described in previous reports (12, 37, 38). *SI Materials and Methods* provides more details.

**Statistical Analysis of Slice Electrophysiology Data.** Data are presented as mean  $\pm$  SEM. For Fig. 2, statistical significance, defined as  $P < 0.05$ , was calculated with unpaired nonparametric Wilcoxon rank sum test as appropriate by using KaleidaGraph (Synergy Software). For Figs. 1, 3, and 4, and Fig. S4, statistical analysis was performed by using GraphPad Prism 5 (GraphPad Software) by one-way ANOVA, followed by Bonferroni's post hoc tests.

**Motor Behavior.** All behavioral observations and measurements were performed blind to genotype. Footprint assay, neurological examination, rotarod, open field, wire hang, and grip strength tests were performed as described in *SI Materials and Methods*.

**ACKNOWLEDGMENTS.** We thank Dr. M. Watanabe of Hokkaido University for the generosity for sharing the  $\gamma$ -2 and  $\gamma$ -7 antibodies; Drs. A. Chesler, W. Lu, T. Hnasko, and all members of the R.A.N. laboratory for helpful discussions; and K. Bjorgan for technical support. M.Y. is supported by the Uehara Memorial Foundation. A.C.J. is supported by a postdoctoral fellowship from National Institute of Mental Health (NIMH). R.A.N. is supported by grants from the NIMH.

- Brackenburg WJ, Isom LL (2011) Na channel  $\beta$  subunits: Overachievers of the ion channel family. *Front Pharmacol* 2:53.
- Vacher H, Mohapatra DP, Trimmer JS (2008) Localization and targeting of voltage-dependent ion channels in mammalian central neurons. *Physiol Rev* 88(4):1407–1447.
- Chen L, et al. (2000) Stargazin regulates synaptic targeting of AMPA receptors by two distinct mechanisms. *Nature* 408(6815):936–943.
- Hashimoto K, et al. (1999) Impairment of AMPA receptor function in cerebellar granule cells of ataxic mutant mouse *stargazer*. *J Neurosci* 19(14):6027–6036.
- Coombs ID, Cull-Candy SG (2009) Transmembrane AMPA receptor regulatory proteins and AMPA receptor function in the cerebellum. *Neuroscience* 162(3):656–665.
- Jackson AC, Nicoll RA (2011) The expanding social network of ionotropic glutamate receptors: TARPs and other transmembrane auxiliary subunits. *Neuron* 70(2):178–199.
- Kato AS, Gill MB, Yu H, Nisenbaum ES, Brecht DS (2010) TARPs differentially decorate AMPA receptors to specify neuropharmacology. *Trends Neurosci* 33(5):241–248.
- Milstein AD, Nicoll RA (2008) Regulation of AMPA receptor gating and pharmacology by TARP auxiliary subunits. *Trends Pharmacol Sci* 29(7):333–339.
- Straub C, Tomita S (2012) The regulation of glutamate receptor trafficking and function by TARPs and other transmembrane auxiliary subunits. *Curr Opin Neurobiol* 22(3):488–495.
- Tomita S, et al. (2005) Stargazin modulates AMPA receptor gating and trafficking by distinct domains. *Nature* 435(7045):1052–1058.
- Fukaya M, Yamazaki M, Sakimura K, Watanabe M (2005) Spatial diversity in gene expression for VDCCgamma subunit family in developing and adult mouse brains. *Neurosci Res* 53(4):376–383.
- Kato AS, et al. (2007) New transmembrane AMPA receptor regulatory protein isoform, gamma-7, differentially regulates AMPA receptors. *J Neurosci* 27(18):4969–4977.
- Lein ES, et al. (2007) Genome-wide atlas of gene expression in the adult mouse brain. *Nature* 445(7124):168–176.
- Yamazaki M, et al. (2010) TARPs gamma-2 and gamma-7 are essential for AMPA receptor expression in the cerebellum. *Eur J Neurosci* 31(12):2204–2220.
- Menuez K, Nicoll RA (2008) Loss of inhibitory neuron AMPA receptors contributes to ataxia and epilepsy in *stargazer* mice. *J Neurosci* 28(42):10599–10603.
- Kato AS, Siuda ER, Nisenbaum ES, Brecht DS (2008) AMPA receptor subunit-specific regulation by a distinct family of type II TARPs. *Neuron* 59(6):986–996.
- Bats C, Soto D, Studniarczyk D, Farrant M, Cull-Candy SG (2012) Channel properties reveal differential expression of TARPed and TARPless AMPARs in *stargazer* neurons. *Nat Neurosci* 15(6):853–861.
- Studniarczyk D, Coombs I, Cull-Candy SG, Farrant M (2013) TARP  $\gamma$ -7 selectively enhances synaptic expression of calcium-permeable AMPARs. *Nat Neurosci* 16(9):1266–1274.
- Letts VA, et al. (1998) The mouse *stargazer* gene encodes a neuronal  $Ca^{2+}$ -channel gamma subunit. *Nat Genet* 19(4):340–347.
- Chu PJ, Robertson HM, Best PM (2001) Calcium channel gamma subunits provide insights into the evolution of this gene family. *Gene* 280(1–2):37–48.
- Paternain AV, Morales M, Lerma J (1995) Selective antagonism of AMPA receptors unmasks kainate receptor-mediated responses in hippocampal neurons. *Neuron* 14(1):185–189.
- Jackson AC, Nicoll RA (2011) Stargazin (TARP gamma-2) is required for compartment-specific AMPA receptor trafficking and synaptic plasticity in cerebellar stellate cells. *J Neurosci* 31(11):3939–3952.
- Shi Y, Lu W, Milstein AD, Nicoll RA (2009) The stoichiometry of AMPA receptors and TARPs varies by neuronal cell type. *Neuron* 62(5):633–640.
- Zhang X-M, et al. (2004) Highly restricted expression of Cre recombinase in cerebellar Purkinje cells. *Genesis* 40(1):45–51.
- Kawata S, et al. (2014) Global scaling down of excitatory postsynaptic responses in cerebellar Purkinje cells impairs developmental synapse elimination. *Cell Reports* 8(4):1119–1129.

26. Yan D, Yamasaki M, Straub C, Watanabe M, Tomita S (2013) Homeostatic control of synaptic transmission by distinct glutamate receptors. *Neuron* 78(4):687–699.
27. Heck DH, De Zeeuw CI, Jaeger D, Khodakhah K, Person AL (2013) The neuronal code(s) of the cerebellum. *J Neurosci* 33(45):17603–17609.
28. Kakizawa S, Yamasaki M, Watanabe M, Kano M (2000) Critical period for activity-dependent synapse elimination in developing cerebellum. *J Neurosci* 20(13):4954–4961.
29. Kano M, et al. (1995) Impaired synapse elimination during cerebellar development in PKC gamma mutant mice. *Cell* 83(7):1223–1231.
30. Najafi F, Medina JF (2013) Beyond “all-or-nothing” climbing fibers: Graded representation of teaching signals in Purkinje cells. *Front Neural Circuits* 7:115.
31. Ito M (2013) Error detection and representation in the olivo-cerebellar system. *Front Neural Circuits* 7:1.
32. Aiba A, et al. (1994) Deficient cerebellar long-term depression and impaired motor learning in mGluR1 mutant mice. *Cell* 79(2):377–388.
33. Chen C, et al. (1995) Impaired motor coordination correlates with persistent multiple climbing fiber innervation in PKC gamma mutant mice. *Cell* 83(7):1233–1242.
34. Jun K, et al. (1999) Ablation of P/Q-type Ca(2+) channel currents, altered synaptic transmission, and progressive ataxia in mice lacking the alpha(1A)-subunit. *Proc Natl Acad Sci USA* 96(26):15245–15250.
35. Kashiwabuchi N, et al. (1995) Impairment of motor coordination, Purkinje cell synapse formation, and cerebellar long-term depression in GluR delta 2 mutant mice. *Cell* 81(2):245–252.
36. Madisen L, et al. (2010) A robust and high-throughput Cre reporting and characterization system for the whole mouse brain. *Nat Neurosci* 13(1):133–140.
37. Milstein AD, Zhou W, Karimzadegan S, Bredt DS, Nicoll RA (2007) TARP subtypes differentially and dose-dependently control synaptic AMPA receptor gating. *Neuron* 55(6):905–918.
38. Shi Y, et al. (2010) Functional comparison of the effects of TARPs and cornichons on AMPA receptor trafficking and gating. *Proc Natl Acad Sci USA* 107(37):16315–16319.